Cell

Regulation of Tumor Cell Mitochondrial Homeostasis by an Organelle-Specific Hsp90 Chaperone Network

Byoung Heon Kang,[1] Janet Plescia,[1] Takehiko Dohi,[1] Jack Rosa,[2] Stephen J. Doxsey,[2] and Dario C. Altieri[1,*]
[1]Department of Cancer Biology
[2]Department of Molecular Medicine and the Cancer Center
University of Massachusetts Medical School, Worcester, MA 01605, USA
*Correspondence: dario.altieri@umassmed.edu
DOI 10.1016/j.cell.2007.08.028

SUMMARY

Molecular chaperones, especially members of the heat shock protein 90 (Hsp90) family, are thought to promote tumor cell survival, but this function is not well understood. Here, we show that mitochondria of tumor cells, but not most normal tissues, contain Hsp90 and its related molecule, TRAP-1. These chaperones interact with Cyclophilin D, an immunophilin that induces mitochondrial cell death, and antagonize its function via protein folding/refolding mechanisms. Disabling this pathway using novel Hsp90 ATPase antagonists directed to mitochondria causes sudden collapse of mitochondrial function and selective tumor cell death. Therefore, Hsp90-directed chaperones are regulators of mitochondrial integrity, and their organelle-specific antagonists may provide a previously undescribed class of potent anticancer agents.

INTRODUCTION

Heat shock protein 90 (Hsp90) is an essential ATPase-directed molecular chaperone (Young et al., 2004) that assists in protein folding quality control (Young et al., 2001), maturation of client proteins (Pearl and Prodromou, 2006), and protein trafficking among specialized subcellular compartments (Young et al., 2003). Because of its restricted repertoire of client proteins, typically kinases and signaling molecules, Hsp90 occupies a unique nodal role in cellular homeostasis, overseeing cell proliferation and cell-survival mechanisms (Pearl and Prodromou, 2006). These properties are commonly exploited in cancer where Hsp90 is not only upregulated (Isaacs et al., 2003), but its ATPase activity is also increased by approximately 100-fold, as compared to that of normal tissues (Kamal et al., 2003).

In tumor cells, Hsp90 is thought to orchestrate a broad cell-survival program (Isaacs et al., 2003; Whitesell and Lindquist, 2005), which has been linked to stabilization of cell viability effectors (Sato et al., 2000), adaptation to unfavorable environments (Beere, 2004), and inhibition of mitochondria-initiated apoptosis (Pandey et al., 2000). Because of its multiple roles as a cancer gene, and the potential "drugability" of its ATPase pocket, Hsp90 has been pursued for novel cancer therapeutics (Isaacs et al., 2003), and a small molecule Hsp90 antagonist derived from geldanamycin (GA), i.e., 17-allylamino-demethoxygeldanamycin (17-AAG) (Neckers and Ivy, 2003), has entered clinical testing in cancer patients (Collins and Workman, 2006). However, the response to this agent proved difficult to interpret. This reflected a modest anticancer activity (Drysdale et al., 2006) that was inconsistent with a predicted essential role of Hsp90 in tumor maintenance (Neckers and Ivy, 2003), paradoxical activation of oncogenic kinases (Koga et al., 2006), induction of antiapoptotic mechanisms (Beere, 2004), and increased metastatic dissemination (Price et al., 2005). It is therefore clear that Hsp90 homeostasis in tumors involves cell-survival mechanisms that escape inhibition by current ATPase antagonists, and unraveling these pathways has become a priority to identify more effective anticancer agents.

Mitochondria play a critical role in cell survival and cell death (Green and Kroemer, 2004). Dysfunction and loss of integrity of these organelles are molecular prerequisites of multiple cell death pathways, characterized by increased permeability of the inner mitochondrial membrane, loss of membrane potential, swelling of the matrix, and ultimately rupture of the outer membrane with release of apoptogenic proteins, i.e., cytochrome *c*, in the cytosol (Green and Kroemer, 2004). How this process of "mitochondrial permeability transition" is regulated is not completely understood (Green and Kroemer, 2004), as components of a "permeability transition pore," including the voltage-dependent anion channel (VDAC-1), the adenine nucleotide translocator (ANT), or the immunophilin Cyclophilin D (CypD), were found to be either dispensable (Kokoszka et al., 2004; Krauskopf et al., 2006), or implicated in some, but not all, forms of mitochondrial cell death (Baines et al., 2005; Nakagawa et al., 2005). Although therapeutic manipulation of mitochondrial permeability transition may hold promise for novel cancer

therapeutics (Johnstone et al., 2002), it is unclear whether mitochondrial homeostasis is differentially regulated in tumor versus normal cells to make this approach safe and devoid of side effects.

In this study, we investigated mechanisms of Hsp90 cytoprotection in tumors. We found that mitochondria of tumor cells, but not most normal tissues, organize a chaperone network comprising Hsp90, its related molecule, TRAP-1 (Felts et al., 2000), and CypD, which antagonizes mitochondrial permeability transition. Organelle-specific targeting of this pathway causes sudden collapse of mitochondrial integrity and apoptosis selectively in tumor cells.

RESULTS

Hsp90 Chaperones in Mitochondria

We began this study by asking whether Hsp90 contributed to mitochondrial cell death pathways, especially in tumors. An Hsp90-related molecule known as TRAP-1 that binds ATPase pocket antagonists has been reported in mitochondria (Cechetto and Gupta, 2000; Felts et al., 2000). Consistent with this, an antibody to TRAP-1 detected an abundant ~75 kDa immunoreactive band in purified mitochondria from various tumor cells (Figure 1A, top). Conversely, TRAP-1 was expressed at very low levels in mitochondria isolated from normal mouse tissues (Figure 1A, bottom) and was absent in the cytosol of tumor or normal cells (Figure 1A and data not shown) (Chen et al., 1996). We next looked at TRAP-1 expression in primary tumor specimens and their matched normal tissues in vivo. By immunohistochemistry, TRAP-1 was intensely expressed in tumor cells of adenocarcinoma of the pancreas (Figure 1C), breast (Figure 1E), colon (Figure 1G), and lung (Figure 1I). Conversely, normal matched epithelia contained very low levels of TRAP-1 (Figures 1B, 1D, 1F, and 1H), and IgG did not stain normal or tumor tissues (data not shown).

Next, we asked whether Hsp90 was also expressed in mitochondria. In addition to cytosol, an abundant pool of Hsp90 was detected by western blotting in mitochondria of various tumor cells (Figure 1J). Accordingly, an antibody to Hsp90 labeled purified tumor mitochondria (26.6 ± 4.1 gold particles/mitochondria, n = 13) by electron microscopy (Figure 1K), whereas IgG was unreactive (1.1 ± 0.33 gold particles/mitochondria, n = 13; $p < 0.0001$) (Figure 1L). To confirm this localization of Hsp90 chaperones, we next checked the purity of our mitochondrial preparations. Mitochondria isolated from HeLa cells contained TRAP-1 and Hsp90 but not proteins of the endoplasmic reticulum (calnexin) or cytosol (GAPDH) and very low amounts of Lamp-1, a lysosomal marker (Figure 1M). Then, we tested whether Hsp90 was actively imported in mitochondria. ^{35}S-labeled Hsp90 accumulated inside isolated brain mitochondria, and this reaction was abolished by the uncoupler, valinomycin (Figure 2A). Similar results were obtained with ^{35}S-PiC, a mitochondrial phosphate carrier used as a control for the import reaction (Figure 2A).

To map the submitochondrial localization of Hsp90, we first degraded the outer membrane proteins, including Bcl-2, with proteinase K (PK). This did not reduce Hsp90 reactivity in mitochondria (Figure S1), suggesting that it was protected from proteolysis. Conversely, permeabilization of the outer membrane with digitonin released Hsp90 from mitochondrial pellets into the supernatant, whereas matrix-associated mt-Hsp70 was unaffected (Figure 2B). Next, we mechanically disrupted the outer membrane in the absence of sucrose, which completely depleted Smac from the intermembrane space, without affecting CypD in the matrix (Figure 2C). Under these conditions, Hsp90 levels were only partially reduced (Figure 2C), suggesting altogether that it localized to both the matrix and the mitochondrial intermembrane space. To validate this, we next used a submitochondrial fractionation protocol that allows the isolation of the outer membrane (OM), the intermembrane space (IMS), the inner membrane (IM), and the matrix (MA). Consistent with the digitonin/proteinase K mapping data (Figures 2B and 2C), Hsp90 was present in both the IMS and the mitochondrial matrix (Figure 2D).

Similar to TRAP-1, mitochondrial Hsp90 was not expressed in normal mouse tissues, except for brain and testis (Figures S1 and 2E). Conversely, cytosolic Hsp90 was ubiquitous in normal and tumor cells (Figure 2E). Analysis of human cells gave comparable results, with Hsp90 and TRAP-1 abundantly present in tumor cells but expressed at low levels in three normal fibroblast cell types (Figure 2F). This was not due to a global reduction in chaperone levels because only the mitochondrial pools of Hsp90 and TRAP-1 were reduced in normal cells, whereas cytosolic Hsp90 was comparably expressed in normal or tumor cells (Figure 2G).

Mitochondrial Hsp90 Chaperones Regulate Permeability Transition

To probe the function of Hsp90 chaperones in mitochondria, we used two ATPase pocket antagonists currently explored as anticancer agents, the small molecule GA derivative, 17-AAG (Isaacs et al., 2003), and the peptidomimetic Shepherdin, which contains an *Antennapedia* helix III homeodomain cell-penetrating sequence (Plescia et al., 2005). Fluorescein-conjugated Shepherdin accumulated inside purified tumor mitochondria (Figure 3A), whereas no fluorescence was detected for Shepherdin lacking the *Antennapedia* sequence (Figure 3B), or in the absence of mitochondria (Figure 3C). A fluorescein-conjugated cell-permeable scrambled peptidomimetic also accumulated in isolated mitochondria (Figure 3D), quantitatively indistinguishably from Shepherdin (Figure 3E). Analysis of submitochondrial compartments revealed that Shepherdin accumulated in the IMS, the IM, and the MA (Figure 3F). This localization was entirely dependent on the *Antennapedia* peptide because Shepherdin lacking this sequence was not found in mitochondria (Figure 3F).

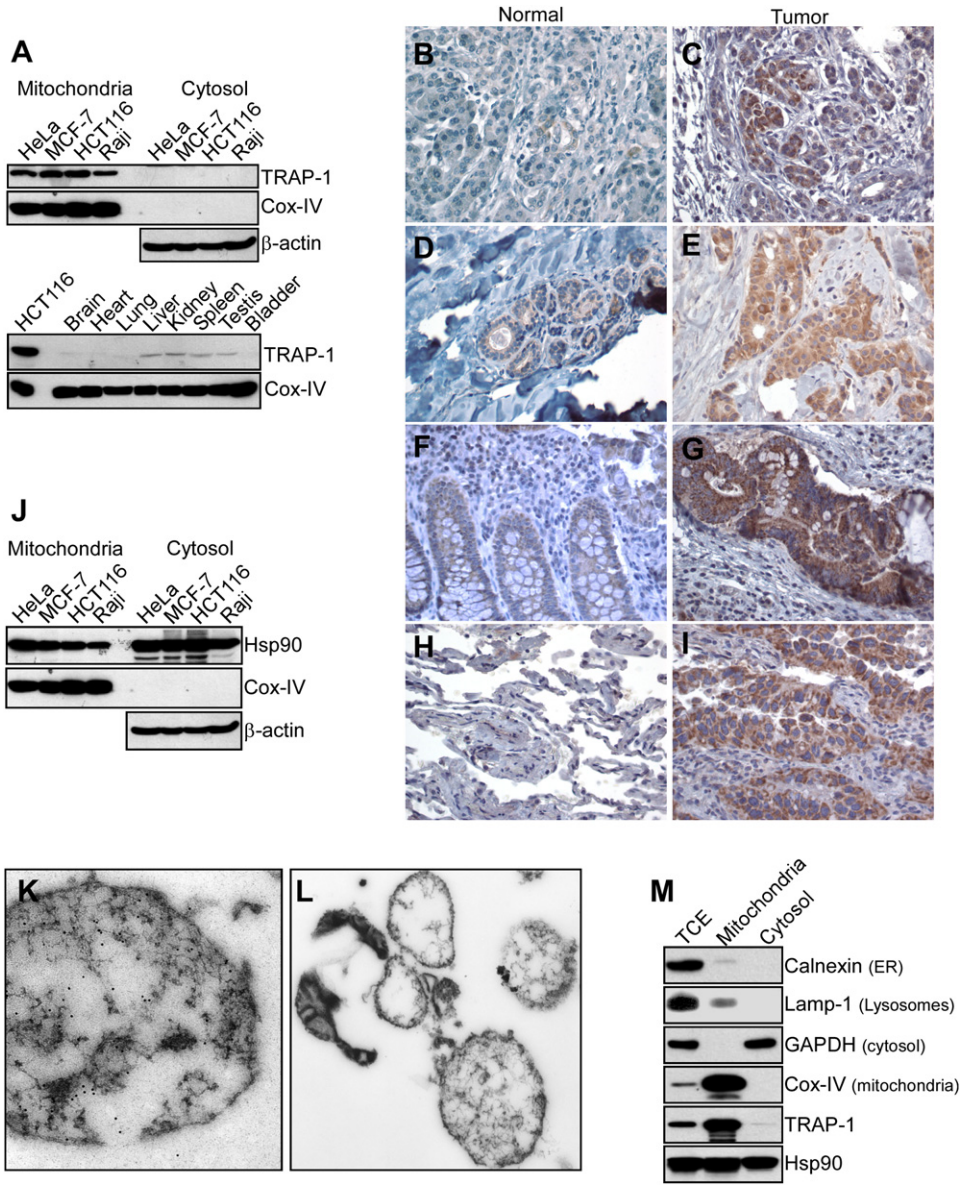

Figure 1. Mitochondrial Hsp90 Chaperones

(A) Differential mitochondrial localization of TRAP-1. Cytosolic or mitochondrial extracts of tumor cells (top) or mitochondria from normal mouse organs (bottom) were analyzed by western blotting.

(B–I) In vivo expression. Tissue specimens of normal pancreas (B), breast (D), colon (F), or lung (H) or cases of adenocarcinoma of pancreas (C), breast (E), colon (G), or lung (I) were stained by immunohistochemistry with an antibody to TRAP-1. Magnification ×400.

(J) Mitochondrial Hsp90 in tumor cells. The indicated tumor cell lines were fractionated in mitochondria or cytosolic extracts and analyzed by western blotting.

(K and L) Electron microscopy. HeLa cell mitochondria were labeled with an antibody to the N domain of Hsp90 (K) or IgG (L), stained with gold-conjugated secondary reagent, and analyzed by electron microscopy. Magnification ×52,000; ×28,000.

(M) Purity of isolated subcellular fractions. Total cytosol extracts (TCE), isolated mitochondria (PK-treated), or cytosolic extracts from HeLa cells were analyzed by western blotting.

Next, we asked whether Shepherdin directly bound Hsp90 molecules in mitochondria in vivo. Fractionation of Raji mitochondrial extracts over Shepherdin-Sepharose resulted in the specific elution of both TRAP-1 and Hsp90 (Figure 3G, top), whereas no bands were affinity-purified by the scrambled peptidomimetic coupled to Sepharose (Figure 3G, bottom).

When tested on isolated tumor mitochondria, Shepherdin induced sudden loss of mitochondrial membrane potential, in a reaction progressively titrated out at increasing

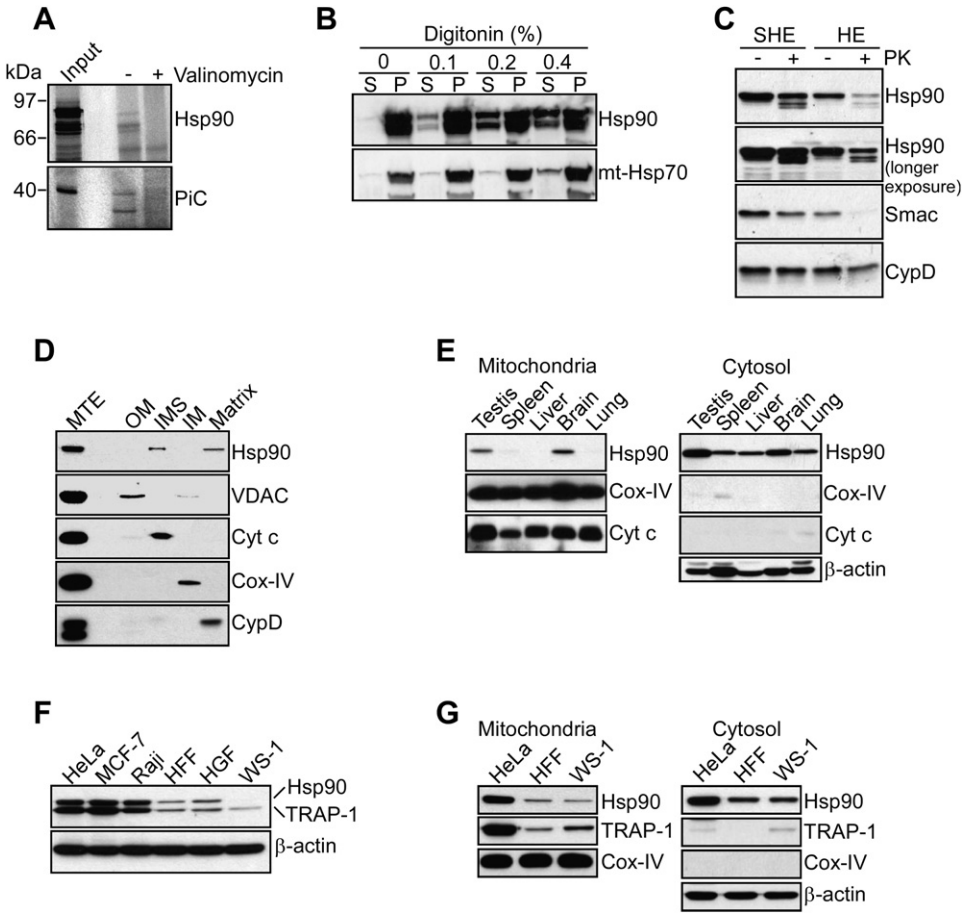

Figure 2. Characterization of Mitochondrial Hsp90

(A) Mitochondrial import. Purified mitochondria were incubated with ^{35}S-Hsp90 or ^{35}S-PiC with (+) or without (–) valinomycin and analyzed by autoradiography.

(B) Digitonin treatment. PK-treated HeLa cell mitochondria were incubated with digitonin, and pellets (P) or supernatants (S) were analyzed by western blotting.

(C) Outer membrane disruption. HeLa cell mitochondria were suspended in buffer with (SHE) or without (HE) sucrose in the presence or absence of PK and analyzed by western blotting.

(D) Submitochondrial fractionation. HeLa cell mitochondrial extracts (MTE) were fractionated in outer membrane (OM), intermembrane space (IMS), inner membrane (IM), and matrix (MA) and analyzed by western blotting.

(E) Differential Hsp90 expression in normal tissues. Mouse organs fractionated in mitochondria (left) or cytosol (right) were analyzed by western blotting.

(F) Comparative analysis of normal versus tumor cell types. Total cell extracts from tumor (HeLa, MCF-7, Raji) or normal (HFF, HGF, WS-1) cells were analyzed by western blotting.

(G) Subcellular fractionations. The indicated normal cell types or HeLa cells were fractionated in mitochondria (left) or cytosolic (right) extracts and analyzed by western blotting.

mitochondria concentrations (Figure 3H). Conversely, Shepherdin did not significantly depolarize normal mitochondria (see below, Figures 4A, 4C, 4E, and 4G), and a scrambled peptidomimetic had no effect on tumor or normal mitochondria (Figure 3H and see below, Figures 4A, 4C, 4E, and 4G). In addition, Shepherdin induced concentration-dependent release of cytochrome *c* from mitochondria isolated from Raji lymphoblastoid cells (Figure 3I) or a primary human sarcoma sample in vivo (Figure 3J), whereas a scrambled peptidomimetic was ineffective (Figures 3I and 3J). In contrast, 17-AAG did not induce cytochrome *c* or Smac release from isolated tumor mitochondria (Figure 3K), and, only at high concentrations (20 μM), it caused a small discharge of mitochondrial cytochrome *c*, but not Smac, in the supernatant (Figure 3L).

Differential Regulation of Mitochondrial Homeostasis in Tumor versus Normal Cell Types

Differently from tumor, i.e., Raji mitochondria (Figure 4A, right), Shepherdin did not depolarize mitochondria isolated from WS-1 normal human fibroblasts (Figure 4A, left). To test whether this reflected a differential

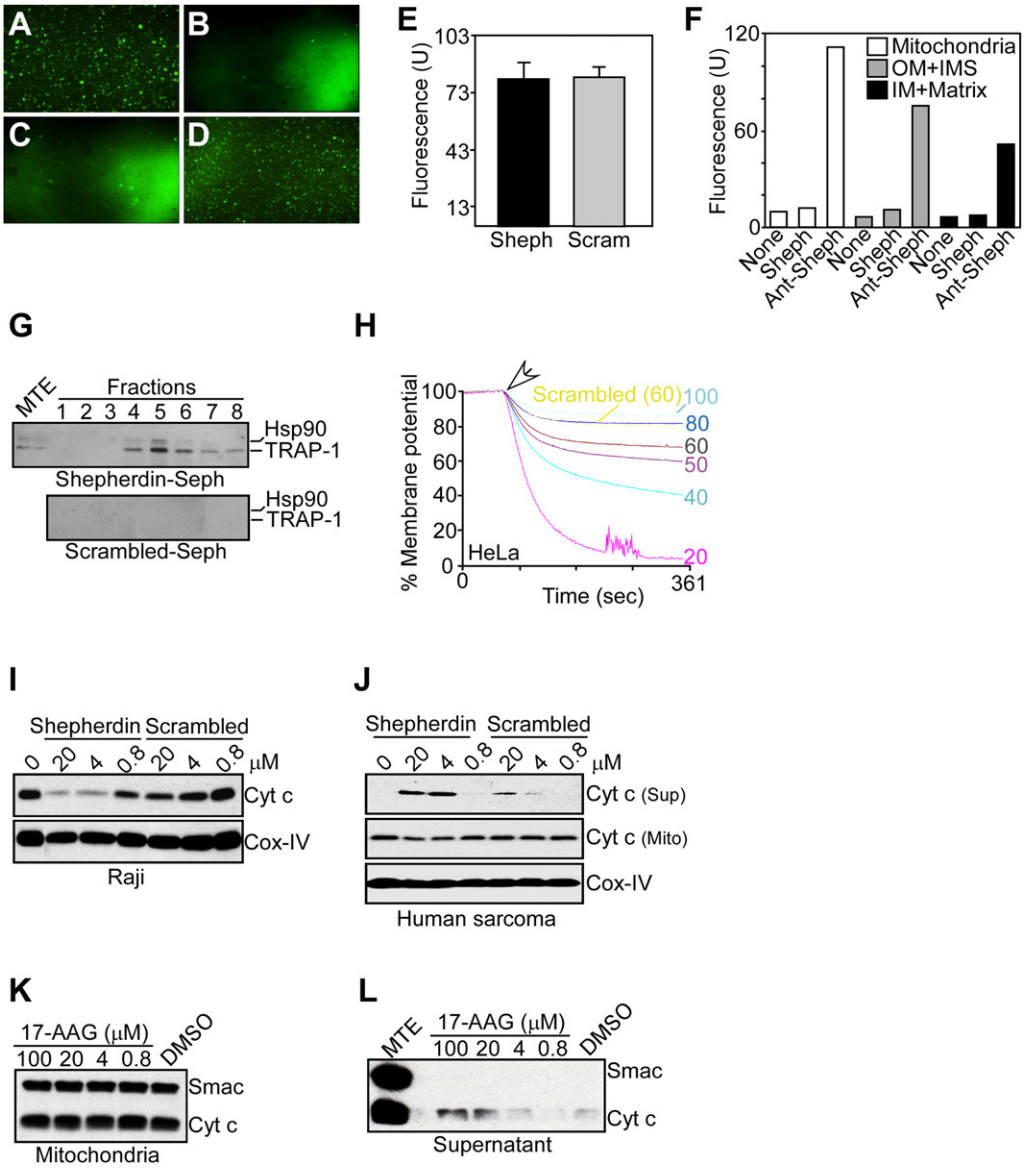

Figure 3. Inhibition of Mitochondrial Hsp90 Induces Permeability Transition

(A–D) Intramitochondrial accumulation. FITC-conjugated Shepherdin (A–C) with (A and C) or without (B) *Antennapedia* cell-penetrating sequence or cell-permeable scrambled peptidomimetic (D) was incubated in the presence (A, B, and D) or absence (C) of HeLa cell mitochondria and analyzed by fluorescence microscopy.

(E) Quantification of intramitochondrial accumulation. Fluorescence intensity was quantified in isolated mitochondrial fractions. Mean ± SEM (n = 3).

(F) Submitochondrial fractions. HeLa cell mitochondria (white bars) incubated with FITC-conjugated Shepherdin without (Sheph) or with *Antennapedia* cell-penetrating sequence (Ant-Sheph) were fractionated in OM+IMS (gray bars) or IM+matrix (black bars) extracts and analyzed for fluorescence intensity. None, untreated.

(G) Affinity chromatography. Raji mitochondrial extracts (MTE) were fractionated over Shepherdin-Sepharose (top) or scrambled peptidomimetic-Sepharose (bottom) beads, and eluted fractions were analyzed by western blotting.

(H) Mitochondrial membrane potential. Increasing concentrations (μg) of TMRM-loaded HeLa cell mitochondria were incubated with Shepherdin and analyzed for changes in fluorescence emission. A scrambled peptidomimetic was incubated with 60 μg of mitochondrial proteins. Arrow, point of addition.

(I–J) Cytochrome *c* release. Mitochondria from Raji cells (I), or a human sarcoma sample (J), were treated with Shepherdin or scrambled peptidomimetic, and mitochondria (Mito) or supernatants (Sup) were analyzed by western blotting.

(K) Effect of 17-AAG. HeLa cell mitochondria were incubated with DMSO or 17-AAG and analyzed by western blotting.

(L) Release of intermitochondrial membrane proteins. Supernatants from 17-AAG-treated HeLa cell mitochondria in (K) were analyzed by western blotting. MTE, mitochondrial extracts.

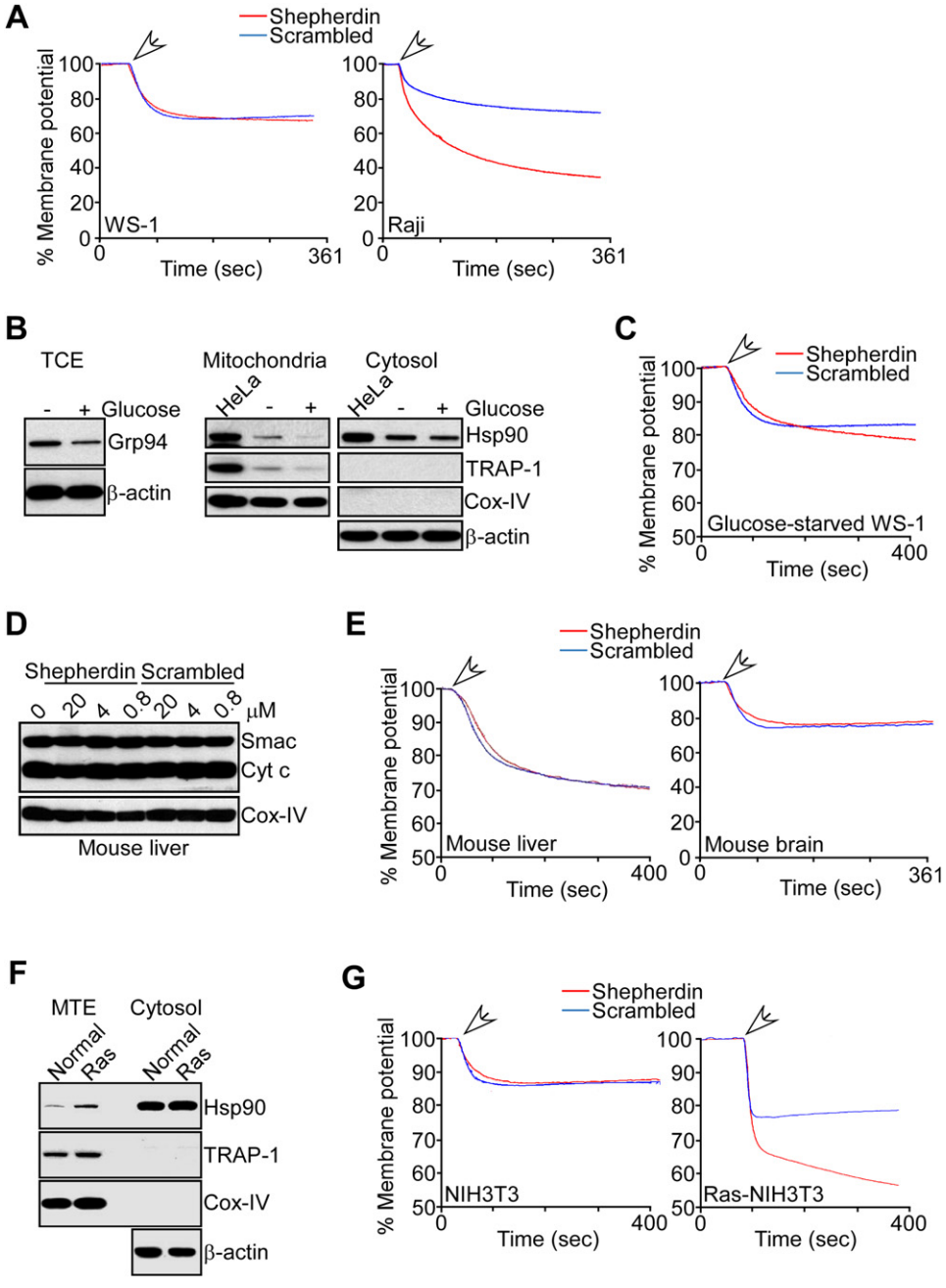

Figure 4. Characterization of Mitochondrial Chaperones in Normal Cells

(A) Mitochondrial membrane potential. TMRM-loaded mitochondria from primary WS-1 fibroblasts (left) or Raji cells (right) were incubated with Shepherdin or scrambled peptidomimetic and analyzed for changes in fluorescence emission.

(B) Glucose deprivation. WS-1 fibroblasts were incubated with (+) or without (−) glucose, and mitochondrial or cytosolic fractions were analyzed by western blotting. HeLa cells were used as control.

(C) Mitochondrial membrane potential. TMRM-loaded mitochondria from glucose-starved WS-1 fibroblasts were incubated with Shepherdin or scrambled peptidomimetic and analyzed for changes in fluorescence emission.

(D) Cytochrome *c* release. Mitochondria from normal mouse liver were incubated with Shepherdin or scrambled peptidomimetic and analyzed by western blotting.

(E) Mitochondrial membrane potential in normal organs. TMRM-loaded mitochondria from normal mouse liver (left) or brain (right) were incubated with Shepherdin or scrambled peptidomimetic and analyzed for changes in fluorescence emission.

(F) Role of oncogenic transformation. Wild-type NIH 3T3 or Ras-transformed NIH 3T3 fibroblasts were fractionated in mitochondria (MTE) or cytosolic extracts and analyzed by western blotting.

modulation of Hsp90 in normal cells, we "stressed" primary fibroblasts by glucose deprivation and checked Hsp90 expression/function. Glucose deprivation of WS-1 fibroblasts increased the levels of the endoplasmic reticulum Hsp90 homolog, Grp94, used as a control (Figure 4B, left). In contrast, there were minimal changes in TRAP-1 or Hsp90 expression in WS-1 mitochondria after glucose deprivation (Figure 4B, right). Accordingly, Shepherdin or scrambled peptidomimetic did not significantly depolarize glucose-deprived WS-1 mitochondria (Figure 4C).

We next carried out experiments on mitochondria isolated from primary tissues in vivo. Shepherdin induced cytochrome *c* release from mitochondria isolated from a $p53^{-/-}$ mouse lymphoma specimen (Figure S2) but had no effect on normal mouse liver mitochondria (Figure 4D). In parallel, Shepherdin or scrambled peptidomimetic did not depolarize mitochondria from normal mouse liver (Figure 4E, left) or brain (Figure 4E, right). To check whether this differential sensitivity was due to neoplastic transformation, we next used normal NIH 3T3 fibroblasts before or after retroviral infection with a Ras mutant oncogene. Normal NIH 3T3 fibroblasts exhibited low levels of mitochondrial Hsp90 (Figure 4F), and Shepherdin did not significantly depolarize their mitochondria (Figure 4G, left). In contrast, Ras-transformed NIH 3T3 fibroblasts exhibited increased recruitment of Hsp90 to mitochondria, whereas changes in TRAP-1 expression were less prominent (Figure 4F), and cytosolic Hsp90 did not change before or after Ras transformation (Figure 4F). Under these conditions, Shepherdin readily depolarized mitochondria from Ras-transformed NIH 3T3 fibroblasts (Figure 4G, right).

Regulation of Tumor Cell Survival by Mitochondrial Hsp90 Chaperones

Because of its ability to trigger mitochondrial dysfunction, we next asked whether Shepherdin selectively killed tumor cells. Fluorescein-conjugated Shepherdin accumulated in the perinuclear area of tumor cells and colocalized with the reactivity of a mitochondrial marker, MitoTracker (Figure 5A). Although competent to accumulate inside isolated mitochondria (Figures 3D and 3E), a cell-permeable scrambled peptidomimetic did not colocalize with MitoTracker in live cells (Figure 5B), thus potentially reflecting nonspecific trapping in various cytosolic membranous compartments in vivo. Accordingly, Shepherdin preferentially accumulated in mitochondrial extracts of treated cells, as compared with scrambled peptidomimetic, whereas both sequences were comparably found in total cell extracts or cytosol fractions (Figure 5C).

Within five minutes of addition, Shepherdin induced loss of mitochondrial membrane potential in tumor cells (Figure 5D) and discharge of mitochondrial cytochrome *c* in the cytosol (data not shown). A cell-permeable scrambled peptidomimetic was without effect (Figure 5D), and, similarly, 17-AAG did not affect mitochondrial membrane potential (Figure 5D) or cytochrome *c* release (Figure 5E) in tumor cells. Within minutes, tumor cells exposed to Shepherdin, but not scrambled peptidomimetic (Movies S1 and S3), exhibited morphological features of apoptosis, including cell shrinkage, membrane blebbing (Movie S2), and fusion/fission of mitochondria (Movie S4) (Figure 5F). Consistent with this, a 1 hr exposure to Shepherdin was sufficient to kill disparate tumor cell types, but not normal primary fibroblasts, in a concentration-dependent manner (Figure 5G). In contrast, a scrambled peptidomimetic had no effect on normal or tumor cells (Figure 5G). Under these conditions, 17-AAG did not affect tumor cell viability, and only a 24 hr treatment with the drug resulted in partial cell killing (Figure 5H).

An Hsp90-Regulated Chaperone Network in Mitochondria

We next looked for molecular interactions of mitochondrial Hsp90 chaperones that may regulate permeability transition in tumor cells. TRAP-1 immunoprecipitated from Raji mitochondria was found in a complex with the immunophilin chaperone CypD (Figure 6A). Inhibition of the peptidyl prolyl-*cis*, *trans*-isomerase activity of CypD with cyclosporine A (CsA) prevented the formation of a CypD-TRAP-1 complex in vivo (Figure 6A). In contrast, inhibition of TRAP-1 ATPase activity with GA had no effect (Figure 6A). Hsp90 immunoprecipitated from mitochondrial extracts also associated with CypD in vivo, and CsA blocked this interaction (Figure 6B). In cell-free pull-down experiments with recombinant proteins, TRAP-1 or Hsp90 directly and reciprocally bound to CypD, and these reactions were abolished by CsA but not GA (Figure S3). In contrast, GST was ineffective (Figure S3). Finally, incubation of GST-CypD with Raji mitochondrial extracts resulted in the isolation of both TRAP-1 and Hsp90, and these interactions were inhibited by CsA, but not GA (Figure 6C).

Molecular Requirements of Hsp90-Directed Mitochondrial Homeostasis

We next carried out experiments to elucidate how Hsp90 chaperones regulate mitochondrial integrity. First, we tested whether CypD contributed to cell death after targeting of mitochondrial Hsp90 molecules. CsA inhibition of CypD completely prevented depolarization of tumor mitochondria induced by Shepherdin (Figure 6D). Consistent with the data above, Shepherdin had no effect on normal liver mitochondria, with or without CsA (Figure S4). In addition, CsA significantly reversed Shepherdin-induced cell death, preserving a 70% cell viability at concentrations of the peptidomimetic (50 μM) that produce complete cell

(G) Mitochondrial membrane potential in normal or transformed fibroblasts. TMRM-loaded mitochondria from NIH 3T3 (left) or Ras-transformed NIH 3T3 (right) fibroblasts were incubated with Shepherdin or scrambled peptidomimetic and analyzed for changes in fluorescence emission. For panels (A), (C), (E), and (G), arrows indicate the points of addition.

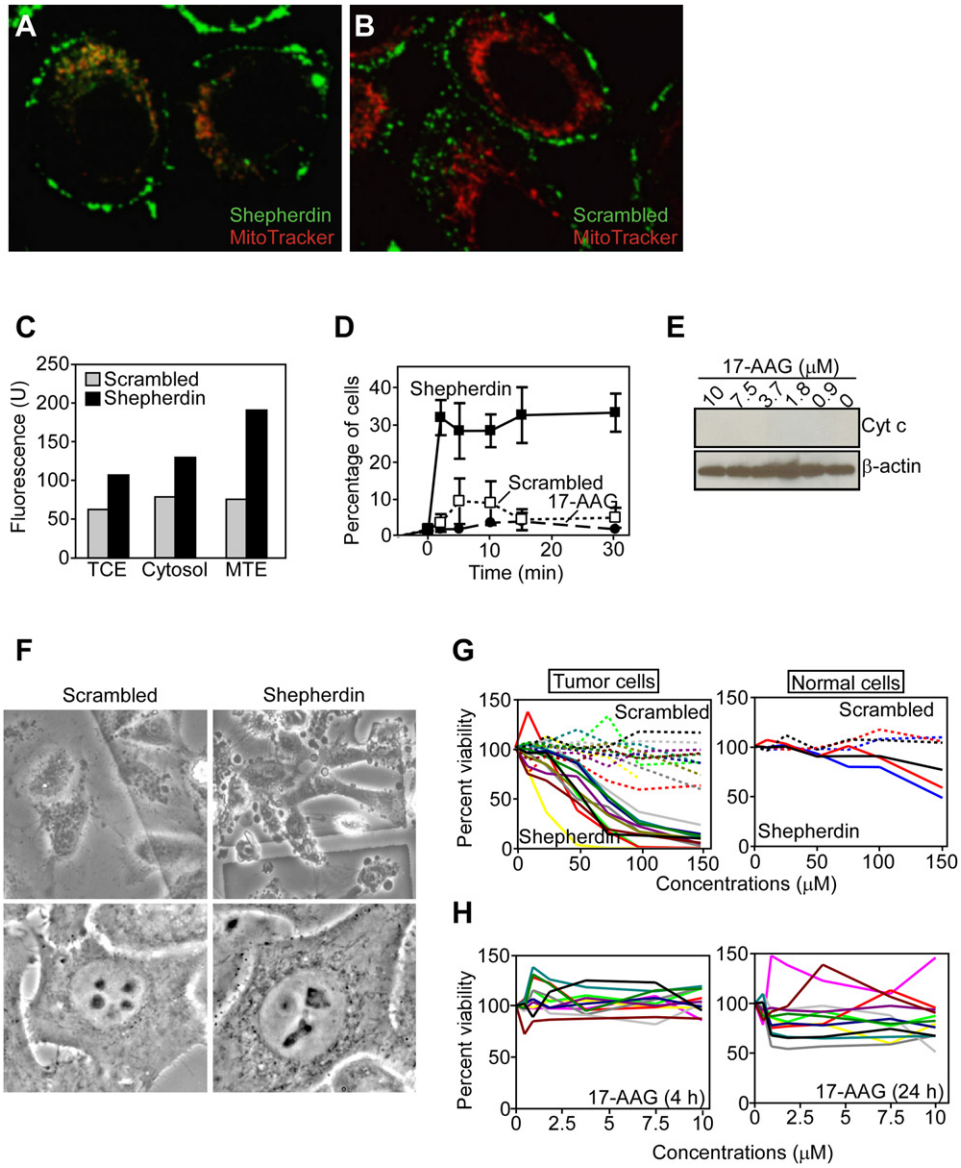

Figure 5. Differential Effects of Hsp90 Inhibitors on Mitochondrial Dysfunction and Tumor Cell Death

(A and B) Confocal microscopy. HeLa cells were double-labeled for mitochondria (MitoTracker) and FITC-conjugated Shepherdin (A) or cell-permeable scrambled peptidomimetic (B) and analyzed by image merging.

(C) Quantification of subcellular accumulation. HeLa cells loaded with FITC-conjugated Shepherdin or scrambled peptidomimetic were fractionated in total cell extracts (TCE), cytosolic extracts, or mitochondrial extracts (MTE) and analyzed for fluorescence intensity.

(D) Mitochondrial membrane potential. JC-1-loaded Raji cells treated with Shepherdin (solid line), 17-AAG (broken line), or scrambled peptidomimetic (dotted line) were analyzed by flow cytometry. Mean ± SEM (n = 4).

(E) Cytochrome *c* release. Cytosolic extracts from 17-AAG-treated HeLa cells were analyzed by western blotting.

(F) Timelapse videomicroscopy. HeLa cells treated with Shepherdin or scrambled peptidomimetic were imaged for cellular morphology of apoptosis (top) or mitochondria fusion/fission (bottom).

(G) Selectivity of Shepherdin-induced tumor cell killing. Tumor (left) or normal (right) cells were incubated with Shepherdin (solid lines) or scrambled peptidomimetic (broken lines), and cell viability was quantified by MTT.

(H) Effect of 17-AAG on tumor cell killing. Tumor cells were incubated with 17-AAG for 4 hr (left) or 24 h (right) and analyzed for cell viability by MTT. For (G) and (H), data are the mean of two independent experiments. The tumor cell types are HeLa (black), MCF-7 (brown), A431 (dark green), PC3 (light green), H460 (blue), H1975 (purple), DU145 (blue green), HCT116 (light gray), MDA-MB-231 (dark gray), Raji (red), HL-60 (bright green), and U937 (yellow). The normal fibroblast cell types are WS-1 (black), HGF (red), and HFF (blue).

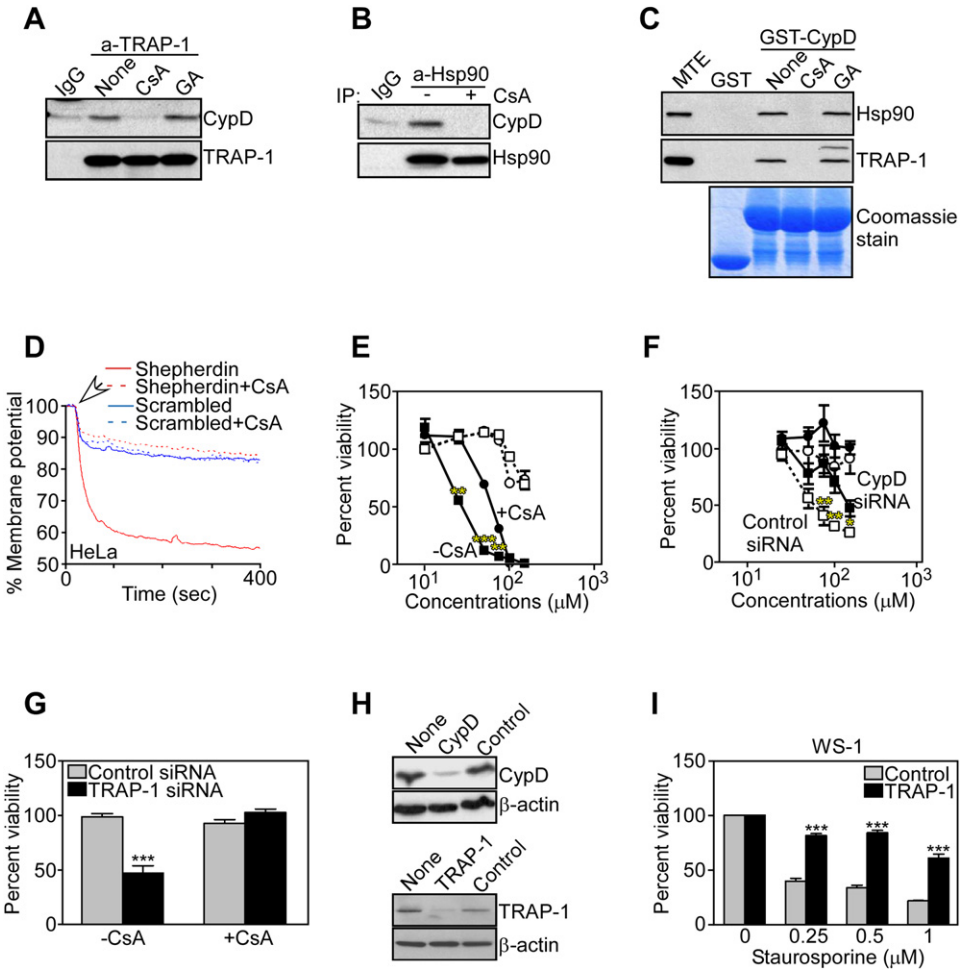

Figure 6. A CypD-Chaperone Complex Regulates Tumor Cell Mitochondrial Permeability Transition

(A) TRAP-1 immunoprecipitation. Raji mitochondrial extracts treated with CsA or GA were immunoprecipitated with an antibody to TRAP-1 or IgG, followed by western blotting.

(B) Hsp90 immunoprecipitation. Raji mitochondrial extracts treated with (+) or without (–) CsA were immunoprecipitated with an antibody to Hsp90 or IgG, followed by western blotting.

(C) In vivo capture assay. GST or GST-CypD was incubated with Raji mitochondrial extracts with or without CsA or GA, followed by western blotting and Coomassie staining.

(D) Mitochondrial membrane potential. TMRM-loaded HeLa cell mitochondria were treated with Shepherdin or scrambled peptidomimetic with (broken lines) or without (solid lines) CsA. Data are from a representative experiment (n = 3). Arrow, point of addition.

(E) Effect of CsA on Shepherdin-induced tumor cell killing. HeLa cells treated with Shepherdin (solid symbols) or scrambled peptidomimetic (open symbols) with (circles) or without (squares) CsA were analyzed by MTT. Mean ± SEM of triplicates of a representative experiment. **p = 0.0012-0.0037; ***p < 0.0001.

(F) CypD knockdown. HeLa cells transfected with nontargeted (open symbols) or CypD-directed siRNA (solid symbols) were treated with Shepherdin (squares) or scrambled peptidomimetic (circles) and analyzed by MTT. Mean ± SEM (n = 4). **p = 0.0074–.0099; *p = 0.029.

(G) TRAP-1 knockdown. HeLa cells were transfected with control nontargeted or TRAP-1-directed siRNA with or without CsA and analyzed by MTT. Mean ± SEM of replicates of two independent experiments. ***p < 0.0001.

(H) Analysis of targeted cells. HeLa cells transfected with nontargeted (control) or CypD- (top) or TRAP-1-directed (bottom) siRNA were analyzed by western blotting. None, nontransfected.

(I) TRAP-1 cytoprotection. Normal WS-1 fibroblasts were transfected with pcDNA3 or TRAP-1 cDNA, treated with staurosporine, and analyzed by MTT. Mean ± SEM of three independent experiments. ***p < 0.0001.

killing in untreated cultures (Figure 6E). To determine whether the protective effect of CsA was specific, we next acutely ablated its target, CypD, by small interfering RNA (siRNA) and analyzed the effect of Shepherdin on these cells. siRNA ablation of CypD effectively prevented Shepherdin-induced tumor cell killing in a reaction quantitatively similar to CsA (Figure 6F). In contrast, a scrambled peptidomimetic had no effect on cell viability, with or without CsA (Figure 6E), or in cultures transfected with nontargeted or CypD-directed siRNA (Figure 6F).

To determine which mitochondrial Hsp90 molecule antagonized CypD, we next acutely ablated TRAP-1 expression, which is solely present in mitochondria, and studied its effect on cell viability. TRAP-1 silencing reduced HeLa cell viability by approximately 50%, as compared with nontargeted siRNA, in a reaction completely reversed by CsA (Figure 6G). In control experiments, TRAP-1- or CypD-directed siRNA reduced the expression of their respective target molecules, whereas nontargeted siRNA had no effect (Figure 6H). As a corollary experiment, we next transfected TRAP-1 in normal human fibroblasts, which express very low levels of this protein (Figures 2F and 2G), and tested their resistance to apoptosis. Expression of TRAP-1 in WS-1 (Figure 6I) or HFF (Figure S5) fibroblasts strongly counteracted apoptosis induced by various concentrations of staurosporine, in agreement with recent observations (Pridgeon et al., 2007), whereas control transfectants were ineffective.

Design and Chemical Synthesis of Mitochondria-Directed GA

Although Shepherdin induced permeability transition and triggered selective tumor cell death, 17-AAG had no effect on mitochondrial integrity (Figures 3K and 3L) and exhibited modest anticancer activity (Figure 5H). To reconcile these discrepancies between Hsp90 antagonists, we hypothesized that 17-AAG was unable to accumulate inside mitochondria and thus inhibit mitochondrial Hsp90 chaperones. Accordingly, fluorescein-conjugated GA failed to accumulate in isolated tumor cell mitochondria (Figure S6A). To overcome this, we coupled by thioether linkages a variant of 17-AAG, 17-(3-(4-Maleimidobutyrcarboxamido)propylamino)-demethoxygeldanamycin (17-GMB-APA-GA) (Figures S6B and S6C), to the *Antennapedia* peptide (Ant), which delivers Shepherdin inside mitochondria (Figure 3F). When conjugated to FITC, this new compound, Ant-GA (Figures S6B and S6C), readily accumulated inside isolated tumor mitochondria, whereas no signal was detected in the absence of mitochondria (Figure S6A). Pretreatment with proteinase K abolished the intramitochondrial accumulation of Ant-GA (Figure S6A). In contrast, addition of proteinase K after Ant-GA incubation with mitochondria was ineffective (Figure S6A), indicating that the compound was protected from proteolysis. Tumor cells exposed to Ant-GA exhibited degradation of Akt, an Hsp90 client protein (Figure S6D), demonstrating that the new compound inhibited the chaperone ATPase activity in vivo, indistinguishably from the uncoupled mixture of Ant and GA (GA/Ant).

Induction of Mitochondrial Permeability Transition and Selective Tumor Cell Death by Ant-GA

We next asked whether mitochondria-directed Ant-GA recapitulated the effect of Shepherdin on mitochondrial permeability transition and tumor cell killing. When added to isolated tumor mitochondria, Ant-GA induced sudden loss of mitochondrial membrane potential in a reaction progressively attenuated at increasing mitochondria concentrations (Figure 7A). Similar to Shepherdin, CsA completely reversed Ant-GA-induced mitochondrial membrane depolarization (Figure 7B), reinforcing a role of CypD in this pathway. In addition, Ant-GA was selective for tumor cells and triggered cytochrome *c* release from isolated tumor mitochondria (Figure 7C, top) but did not affect the membrane potential of normal brain mitochondria, with or without CsA (Figure 7B), or the cytochrome *c* content of normal liver mitochondria (Figure 7C, bottom). Within the same time of exposure, the uncoupled mixture of GA/Ant, or GA alone, had no significant effect on normal or tumor mitochondrial membrane potential (Figure 7B) or cytochrome *c* release (Figure 7C). Treatment with Ant-GA, but not GA alone or the uncoupled Ant/GA mixture, resulted in rapid (~2 hr) and concentration-dependent tumor cell killing (Figure 7D). In contrast, none of the compounds decreased the viability of various normal human fibroblasts (Figure 7E). Finally, tumor cell killing induced by Ant-GA had the hallmarks of apoptosis with increased caspase activity and was indistinguishable in tumor cells either containing or lacking p53 (Figure 7F). In contrast, the uncoupled mixture GA/Ant did not induce apoptosis in $p53^{+/+}$ or $p53^{-/-}$ cells (Figure 7F).

DISCUSSION

In this study, we have shown that tumor cells organize a mitochondrial chaperone network, which involves Hsp90, its related molecule, TRAP-1, and the immunophilin CypD. This complex maintains mitochondrial homeostasis and antagonizes the function of CypD in permeability transition. Conversely, inhibition of mitochondrial Hsp90 chaperones with a novel class of mitochondria-directed ATPase antagonists causes sudden loss of mitochondrial membrane potential, release of cytochrome *c*, and massive death of tumor but not normal cells.

The identification of an Hsp90 chaperone network in mitochondria fits well with an emerging paradigm that the homeostatic functions of these molecules are orchestrated in specialized subcellular microenvironments. This relies on organelle-specific cofactors (Young et al., 2003) and chaperones (Panaretou et al., 2002) but also on compartmentalized ATPase-directed "Hsp90-like" molecules, including Grp94 in the endoplasmic reticulum (Loo et al., 1998) and TRAP-1 in mitochondria (Cechetto and Gupta, 2000; Felts et al., 2000). Accordingly, an Hsp90 chaperone network oversees protein folding quality control at the endoplasmic reticulum (Young et al., 2001), trafficking of signaling molecules at the plasma membrane (Garcia-Cardena et al., 1998), delivery of preproteins to mitochondria (Young et al., 2003), assembly and disassembly of cytoskeletal proteins in the cytosol (Barral et al., 2002), and disassembly of transcriptional complexes in the nucleus (Freeman and Yamamoto, 2002). Although the exact mechanism(s) of how Hsp90 chaperones are imported in mitochondria remains to be fully elucidated, this may involve the presence of a cleavable mitochondrial targeting sequence in TRAP-1 (Felts et al., 2000) and potential

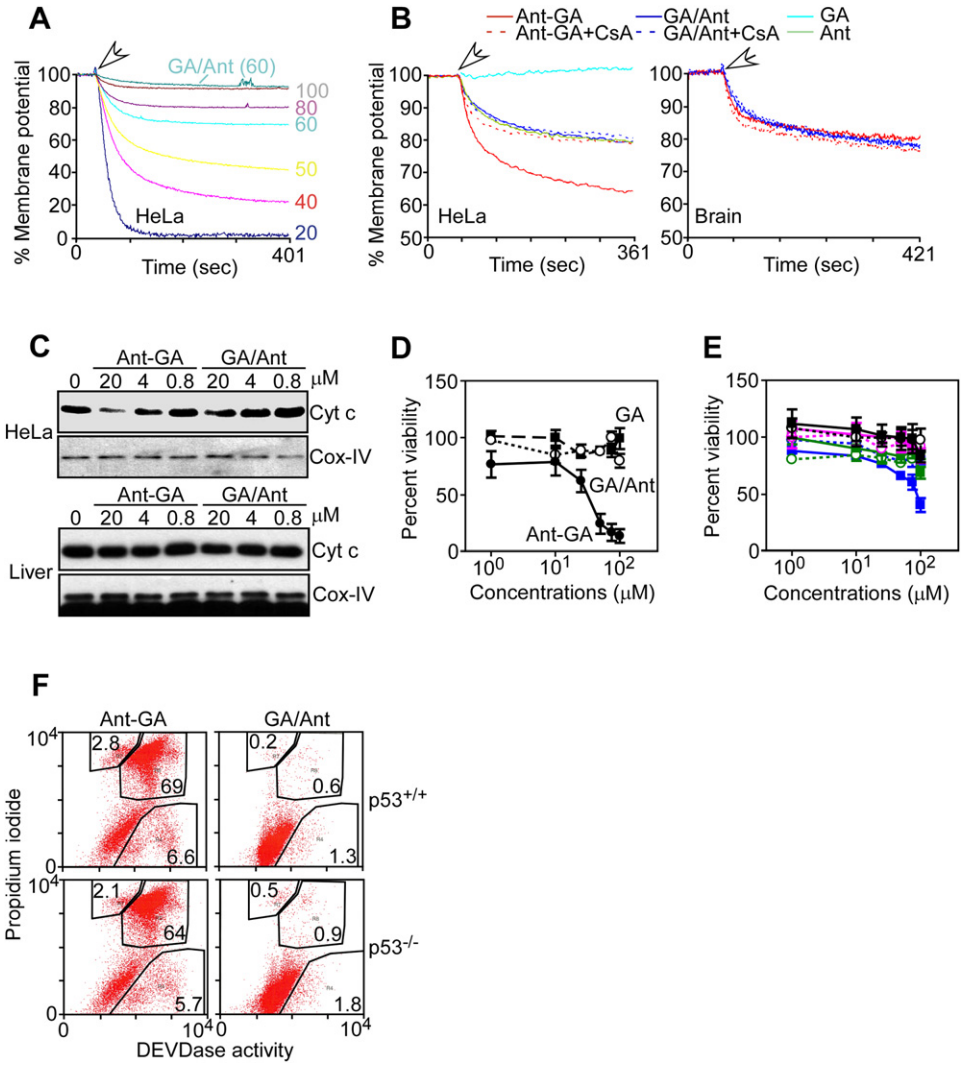

Figure 7. Ant-GA Induction of Mitochondrial Permeability Transition and Tumor Cell Death

(A) Mitochondrial membrane potential. Increasing concentrations (μg) of TMRM-loaded HeLa cell mitochondria were incubated with Ant-GA and analyzed for changes in fluorescence emission. The uncoupled mixture GA/Ant was incubated with 60 μg of isolated mitochondria.

(B) Effect of CsA. TMRM-loaded HeLa cell (left) or mouse brain (right) mitochondria were incubated with the various compounds, with or without CsA, and analyzed for changes in fluorescence emission. Data are from a representative experiment (n = 3). For (A) and (B), arrows indicate the points of addition.

(C) Cytochrome *c* release. Mitochondria from HeLa cells (top) or mouse liver (bottom) were incubated with Ant-GA or the uncoupled mixture of GA/Ant and analyzed by western blotting.

(D) Tumor cell killing. HeLa cells were incubated with the various compounds and analyzed by MTT. Data are the means ± SEM of three independent experiments.

(E) Effect on normal cells. Primary WS-1 (black), HGF (purple), or HFF (green) fibroblasts were treated with Ant-GA (solid squares) or the uncoupled mixture of GA/Ant (open circles) and analyzed by MTT. Prostate cancer PC3 cells (blue) were used as control. Data are the means ± SEM of three independent experiments.

(F) p53-independent induction of apoptosis. $p53^{+/+}$ (top) or $p53^{-/-}$ (bottom) HCT116 cells were treated with the various compounds and analyzed for DEVDase activity and propidium iodide staining by flow cytometry. The percentage of cells in each quadrant is indicated.

molecular interactions between Hsp90 and the mitochondrial import receptor, Tom70 (Young et al., 2003).

In mitochondria, Hsp90 chaperones establish a set of CsA-sensitive molecular interactions with the matrix immunophilin CypD and antagonize its ability to induce mitochondrial permeability transition and cell death (Green and Kroemer, 2004). Because TRAP-1 knockdown only partially removed this protective effect and induced ~50% cell killing, it seems likely that both Hsp90 chaperones are required to oppose CypD function and maintain mitochondrial homeostasis, potentially via the assembly of independent molecular complexes with CypD

(unpublished data). How CypD mediates mitochondrial permeability transition has been the subject of intense investigation and may involve physical association with pore components (Green and Kroemer, 2004), ANT-independent mechanisms of pore formation (Kokoszka et al., 2004), or remodeling of mitochondrial cristae for full discharge of cytochrome *c* (Scorrano et al., 2002). Regardless, genetic deletion of CypD (Baines et al., 2005; Nakagawa et al., 2005) or inhibition of its peptidyl prolyl-*cis*, *trans*-isomerase activity or molecular conformation by CsA (Kokoszka et al., 2004) abolished mitochondrial permeability transition, especially in response to oxidative stress and Ca^{2+} overload, thus underscoring a critical role in mitochondrial cell death.

The ability of mitochondrial Hsp90 chaperones to antagonize the pore-forming properties of CypD and the requirement of their ATPase activity in this process point to a protective mechanism of protein folding/refolding. Although this model applies well to a canonical view of the permeability transition pore as a defined molecular entity composed of ANT, VDAC, and CypD (Green and Kroemer, 2004), it is also readily, and perhaps even more applicable to an alternative scenario, in which permeability transition is mediated by clusters of misfolded proteins in stress-exposed mitochondria (He and Lemasters, 2002). In this case, mitochondrial Hsp90 chaperones would be ideally positioned to bind the protein clusters, block pore conductance via ATPase-directed protein refolding, and antagonize the Ca^{2+}-induced perturbation of CypD activity potentially responsible for pore opening (He and Lemasters, 2002). Conversely, inhibition of mitochondrial Hsp90 ATPase activity eliminates this protective effect, releasing CypD-mediated permeability transition and execution of mitochondrial cell death.

Importantly, this protective pathway by mitochondrial Hsp90 chaperones appears almost exclusively operational in tumor cells, as opposed to most normal tissues. This selectivity emphasizes how broadly Hsp90-directed protein folding is exploited during oncogenic transformation and is ideally suited to preserve steady-state mitochondrial integrity, elevate the organelle threshold for initiation of cell death (Green and Kroemer, 2004) during cellular or environmental stress (Beere, 2004), and favor drug resistance, which is a trait of Hsp90 in certain model organisms (Cowen and Lindquist, 2005). Conversely, the existence of "tumor-specific" qualitative differences in mitochondrial protein composition and molecular interactions (Mootha et al., 2003) may provide new prospects for the development of selective anticancer agents.

We pursued this concept by designing a new class of mitochondria-directed Hsp90 antagonists, aimed at disabling this organelle-specific protective network. The prototype molecule in this class was Shepherdin, which exhibited marked rapidity of action, potent tumor cell killing, and lack of toxicity for normal tissues in vivo (Plescia et al., 2005). It is now clear that these properties reflect the ability of Shepherdin to penetrate inside mitochondria, bind mitochondrial TRAP-1 and Hsp90, and inhibit their chaperone activity via an ATP competition mechanism (Neckers and Ivy, 2003; Plescia et al., 2005), thus resulting in CypD-mediated cell death. Although the ability of cell-penetrating peptides, i.e., *Antennapedia* helix III, to target cargos to mitochondria has been debated (Torchilin, 2006), this sequence is clearly required to mediate intramitochondrial accumulation of Shepherdin, potentially via electrostatic interactions with the negatively charged mitochondrial matrix. Extending this paradigm, we synthesized a mitochondria-directed variant of 17-AAG carrying the *Antennapedia* peptide, i.e., Ant-GA. Differently from unconjugated 17-AAG, which was not detected in mitochondria and had no effect on permeability transition, Ant-GA efficiently accumulated inside mitochondria and recapitulated the effect of Shepherdin with rapid induction of mitochondrial cell death. The selectivity of these agents, i.e., Shepherdin and Ant-GA, for tumor cells bodes well for their potential clinical development as anticancer agents and may reflect the near exclusive expression of the Hsp90 network in tumor mitochondria, as well as the higher affinity of tumor-associated Hsp90 for ATPase pocket antagonists (Kamal et al., 2003). Accordingly, Ant-GA or Shepherdin showed no toxicity for brain or liver mitochondria, despite the presence of detectable Hsp90 and TRAP-1, respectively, in these organelles.

In summary, Hsp90-directed protein folding/refolding functions as a novel regulatory mechanism of mitochondrial permeability transition (Green and Kroemer, 2004; He and Lemasters, 2002). Although this pathway is selectively exploited in tumor cells to elevate an antiapoptotic threshold, the development of Hsp90 antagonists competent to accumulate in mitochondria may provide a new class of potent and selective anticancer agents, potentially devoid of side effects for normal tissues.

EXPERIMENTAL PROCEDURES

Mitochondria Isolation

Using a Mitochondria Isolation kit (Sigma-Aldrich), crude mitochondria were isolated from mouse brain, liver, a primary lymphoma isolated from a $p53^{-/-}$ mouse, and a case of surgically resected human sarcoma. Cultured cells were washed in TD buffer (135 mM NaCl, 5 mM KCl, 25 mM Tris, pH 7.6), and cell pellets in CaRSB buffer (10 mM NaCl, 1.5 mM $CaCl_2$, 10 mM Tris, pH 7.5, and protease inhibitor) were homogenized in a Dounce grinder and processed as described (Dohi et al., 2004). Crude mitochondrial fractions were collected by centrifugation at 6000 × g for 10 min and suspended in MS buffer containing 210 mM mannitol, 70 mM sucrose, 5 mM Tris, pH 7.6, 5 mM EDTA, and protease inhibitors. In some experiments, samples were incubated with FITC-conjugated Shepherdin for 10 min at 0°C, layered onto 1 M–1.5 M discontinuous sucrose gradient in 10 mM Tris, 5 mM EDTA, pH 7.6, 2 mM DTT, plus protease inhibitors, and centrifuged at 25,000 rpm in a Beckman SW41 rotor for 1 hr at 4°C. The mitochondrial band between 1 M and 1.5 M interface was collected and washed in MS buffer. Protein concentrations were determined with a Protein Assay reagent (BioRad) using BSA (Sigma-Aldrich) as standard. Primary WS-1 fibroblasts were cultured in high-glucose media (DMEM containing 4.5 g/l glucose, Invitrogen) in the presence of 10% FBS and antibiotics. Cells were washed, incubated in no-glucose DMEM

(Sigma) with sodium pyruvate and glutamine for 48 hr at 37°C, and processed for isolation of mitochondrial or cytosolic extracts.

Submitochondrial Fractionation

Submitochondrial fractionation was performed by phosphate swelling-shrinking as described before with minor modifications (Bijur and Jope, 2003; Hovius et al., 1990). Briefly, purified mitochondrial pellets isolated by sucrose step gradient were suspended in swelling buffer (10 mM KH_2PO_4, pH 7.4, and protease inhibitor) and incubated for 20 min at 0°C with gentle mixing. Mitochondria were mixed with equal volume of shrinking buffer (10 mM KH_2PO_4, pH 7.4, 32% sucrose, 30% glycerol, 10 mM $MgCl_2$, and protease inhibitor) for 20 min at 0°C. After centrifugation at 10,000 × g for 10 min, the supernatant was collected as containing outer membrane and intermembrane space fractions (OM&IMS). Pellets were washed three times with 1:1 mixture of swelling-shrinking buffer, suspended in swelling buffer, and sonicated to disrupt the inner membrane, which was collected as containing inner membrane and matrix fractions (IM&MA). OM&IMS and IM&MA were further fractionated by centrifugation at 150,000 × g for 1 hr at 4°C. The pellets were collected as OM and IM fractions, respectively. Supernatants were concentrated using Centricon 10K and Microcon 10K centrifugal filters (Millipore) and collected as IMS and MA fractions, respectively. Mitochondria isolated from HeLa cells or mouse brain (2 μg/μl, 15 μl) were suspended in SHE buffer (250 mM sucrose in HE buffer), diluted in 135 μl of SHE buffer or HE buffer (10 mM HEPES, 1 mM EDTA, pH 7.2), and incubated for 15 min at 0°C with mechanical disruption of the outer membrane by repeated pipetting. After incubation with 50 μg/ml proteinase K (PK, Roche) for 10 min at 0°C, samples were mixed with 1 mM PMSF and centrifuged at 10,000 × g for 10 min. Repartition of mitochondrial proteins from pellets to supernatants in digitonin (0%–0.4%)-permeabilized mitochondria was carried out as described (Dohi et al., 2004).

Mitochondrial Membrane Potential

Raji cells were treated with Shepherdin or control scrambled peptidomimetic (100 μM) or 17-AAG (5 μM), loaded with the mitochondrial membrane potential-sensitive fluorescent dye JC-1, and analyzed for changes in green/red fluorescence ratio by flow cytometry. Alternatively, isolated mitochondria (100 μg) suspended in SB buffer were incubated with 0.1 μM tetramethylrhodamine methyl ester (TMRM), treated with Shepherdin or control scrambled peptidomimetic (0.5–1.5 μM), 17-AAG (1.5 μM), or Ant-GA (1–1.5 μM), with or without CsA (5 μM), and analyzed continuously at 549 nm excitation and 575 nm emission (Photon Technology International, Inc). TMRM-loaded mitochondria in SB buffer were allowed to reach stable fluorescence, which was set as fully polarized state. The fluorescence intensity after treatment with 2 mM $CaCl_2$ was set as minimum membrane potential (fully depolarized state). Changes in fluorescence intensity were plotted as a ratio between maximum and minimum membrane potential. Increasing concentrations (10–100 μg) of TMRM-loaded mitochondria isolated from HeLa or MCF-7 cells were diluted in 3 ml of SB buffer, normalized to a total protein concentration of 500 μg with BSA, and analyzed for changes in membrane potential in response to control or various Hsp90 antagonists.

Supplemental Data

Supplemental Data include Supplemental Experimental Procedures, six figures, and four movies and can be found with this article online at http://www.cell.com/cgi/content/full/131/2/257/DC1/.

ACKNOWLEDGMENTS

We thank Drs. Bert Vogelstein for HCT116 cells, Steve Lyle for tissue analysis, Roger Davis for normal and Ras-transformed NIH 3T3 fibroblasts, and Tracy Levin for electron microscopy. This work was supported by National Institutes of Health grants HL54131, CA90917, and CA78810.

Received: March 7, 2007
Revised: June 14, 2007
Accepted: August 3, 2007
Published: October 18, 2007

REFERENCES

Baines, C.P., Kaiser, R.A., Purcell, N.H., Blair, N.S., Osinska, H., Hambleton, M.A., Brunskill, E.W., Sayen, M.R., Gottlieb, R.A., Dorn, G.W., et al. (2005). Loss of cyclophilin D reveals a critical role for mitochondrial permeability transition in cell death. Nature *434*, 658–662.

Barral, J.M., Hutagalung, A.H., Brinker, A., Hartl, F.U., and Epstein, H.F. (2002). Role of the myosin assembly protein UNC-45 as a molecular chaperone for myosin. Science *295*, 669–671.

Beere, H.M. (2004). "The stress of dying": the role of heat shock proteins in the regulation of apoptosis. J. Cell Sci. *117*, 2641–2651.

Bijur, G.N., and Jope, R.S. (2003). Rapid accumulation of Akt in mitochondria following phosphatidylinositol 3-kinase activation. J. Neurochem. *87*, 1427–1435.

Cechetto, J.D., and Gupta, R.S. (2000). Immunoelectron microscopy provides evidence that tumor necrosis factor receptor-associated protein 1 (TRAP-1) is a mitochondrial protein which also localizes at specific extramitochondrial sites. Exp. Cell Res. *260*, 30–39.

Chen, C.F., Chen, Y., Dai, K., Chen, P.L., Riley, D.J., and Lee, W.H. (1996). A new member of the hsp90 family of molecular chaperones interacts with the retinoblastoma protein during mitosis and after heat shock. Mol. Cell. Biol. *16*, 4691–4699.

Collins, I., and Workman, P. (2006). New approaches to molecular cancer therapeutics. Nat. Chem. Biol. *2*, 689–700.

Cowen, L.E., and Lindquist, S. (2005). Hsp90 potentiates the rapid evolution of new traits: drug resistance in diverse fungi. Science *309*, 2185–2189.

Dohi, T., Beltrami, E., Wall, N.R., Plescia, J., and Altieri, D.C. (2004). Mitochondrial survivin inhibits apoptosis and promotes tumorigenesis. J. Clin. Invest. *114*, 1117–1127.

Drysdale, M.J., Brough, P.A., Massey, A., Jensen, M.R., and Schoepfer, J. (2006). Targeting Hsp90 for the treatment of cancer. Curr. Opin. Drug Discov. Dev. *9*, 483–495.

Felts, S.J., Owen, B.A., Nguyen, P., Trepel, J., Donner, D.B., and Toft, D.O. (2000). The hsp90-related protein TRAP1 is a mitochondrial protein with distinct functional properties. J. Biol. Chem. *275*, 3305–3312.

Freeman, B.C., and Yamamoto, K.R. (2002). Disassembly of transcriptional regulatory complexes by molecular chaperones. Science *296*, 2232–2235.

Garcia-Cardena, G., Fan, R., Shah, V., Sorrentino, R., Cirino, G., Papapetropoulos, A., and Sessa, W.C. (1998). Dynamic activation of endothelial nitric oxide synthase by Hsp90. Nature *392*, 821–824.

Green, D.R., and Kroemer, G. (2004). The pathophysiology of mitochondrial cell death. Science *305*, 626–629.

He, L., and Lemasters, J.J. (2002). Regulated and unregulated mitochondrial permeability transition pores: a new paradigm of pore structure and function? FEBS Lett. *512*, 1–7.

Hovius, R., Lambrechts, H., Nicolay, K., and de Kruijff, B. (1990). Improved methods to isolate and subfractionate rat liver mitochondria. Lipid composition of the inner and outer membrane. Biochim. Biophys. Acta *1021*, 217–226.

Isaacs, J.S., Xu, W., and Neckers, L. (2003). Heat shock protein 90 as a molecular target for cancer therapeutics. Cancer Cell *3*, 213–217.

Johnstone, R.W., Ruefli, A.A., and Lowe, S.W. (2002). Apoptosis: a link between cancer genetics and chemotherapy. Cell *108*, 153–164.

Kamal, A., Thao, L., Sensintaffar, J., Zhang, L., Boehm, M.F., Fritz, L.C., and Burrows, F.J. (2003). A high-affinity conformation of Hsp90 confers tumour selectivity on Hsp90 inhibitors. Nature *425*, 407–410.

Koga, F., Xu, W., Karpova, T.S., McNally, J.G., Baron, R., and Neckers, L. (2006). Hsp90 inhibition transiently activates Src kinase and promotes Src-dependent Akt and Erk activation. Proc. Natl. Acad. Sci. USA *103*, 11318–11322.

Kokoszka, J.E., Waymire, K.G., Levy, S.E., Sligh, J.E., Cai, J., Jones, D.P., MacGregor, G.R., and Wallace, D.C. (2004). The ADP/ATP translocator is not essential for the mitochondrial permeability transition pore. Nature *427*, 461–465.

Krauskopf, A., Eriksson, O., Craigen, W.J., Forte, M.A., and Bernardi, P. (2006). Properties of the permeability transition in VDAC1(−/−) mitochondria. Biochim. Biophys. Acta *1757*, 590–595.

Loo, M.A., Jensen, T.J., Cui, L., Hou, Y., Chang, X.B., and Riordan, J.R. (1998). Perturbation of Hsp90 interaction with nascent CFTR prevents its maturation and accelerates its degradation by the proteasome. EMBO J. *17*, 6879–6887.

Mootha, V.K., Bunkenborg, J., Olsen, J.V., Hjerrild, M., Wisniewski, J.R., Stahl, E., Bolouri, M.S., Ray, H.N., Sihag, S., Kamal, M., et al. (2003). Integrated analysis of protein composition, tissue diversity, and gene regulation in mouse mitochondria. Cell *115*, 629–640.

Nakagawa, T., Shimizu, S., Watanabe, T., Yamaguchi, O., Otsu, K., Yamagata, H., Inohara, H., Kubo, T., and Tsujimoto, Y. (2005). Cyclophilin D-dependent mitochondrial permeability transition regulates some necrotic but not apoptotic cell death. Nature *434*, 652–658.

Neckers, L., and Ivy, S.P. (2003). Heat shock protein 90. Curr. Opin. Oncol. *15*, 419–424.

Panaretou, B., Siligardi, G., Meyer, P., Maloney, A., Sullivan, J.K., Singh, S., Millson, S.H., Clarke, P.A., Naaby-Hansen, S., Stein, R., et al. (2002). Activation of the ATPase activity of hsp90 by the stress-regulated cochaperone aha1. Mol. Cell *10*, 1307–1318.

Pandey, P., Saleh, A., Nakazawa, A., Kumar, S., Srinivasula, S.M., Kumar, V., Weichselbaum, R., Nalin, C., Alnemri, E.S., Kufe, D., and Kharbanda, S. (2000). Negative regulation of cytochrome c-mediated oligomerization of Apaf-1 and activation of procaspase-9 by heat shock protein 90. EMBO J. *19*, 4310–4322.

Pearl, L.H., and Prodromou, C. (2006). Structure and mechanism of the hsp90 molecular chaperone machinery. Annu. Rev. Biochem. *75*, 271–294.

Plescia, J., Salz, W., Xia, F., Pennati, M., Zaffaroni, N., Daidone, M.G., Meli, M., Dohi, T., Fortugno, P., Nefedova, Y., et al. (2005). Rational design of shepherdin, a novel anticancer agent. Cancer Cell *7*, 457–468.

Price, J.T., Quinn, J.M., Sims, N.A., Vieusseux, J., Waldeck, K., Docherty, S.E., Myers, D., Nakamura, A., Waltham, M.C., Gillespie, M.T., and Thompson, E.W. (2005). The heat shock protein 90 inhibitor, 17-allylamino-17-demethoxygeldanamycin, enhances osteoclast formation and potentiates bone metastasis of a human breast cancer cell line. Cancer Res. *65*, 4929–4938.

Pridgeon, J.W., Olzmann, J.A., Chin, L.S., and Li, L. (2007). PINK1 protects against oxidative stress by phosphorylating mitochondrial chaperone TRAP1. PLoS Biol. *5*, e172. 10.1371/journal.pbio.0050172.

Sato, S., Fujita, N., and Tsuruo, T. (2000). Modulation of Akt kinase activity by binding to Hsp90. Proc. Natl. Acad. Sci. USA *97*, 10832–10837.

Scorrano, L., Ashiya, M., Buttle, K., Weiler, S., Oakes, S.A., Mannella, C.A., and Korsmeyer, S.J. (2002). A distinct pathway remodels mitochondrial cristae and mobilizes cytochrome c during apoptosis. Dev. Cell *2*, 55–67.

Torchilin, V.P. (2006). Recent approaches to intracellular delivery of drugs and DNA and organelle targeting. Annu. Rev. Biomed. Eng. *8*, 343–375.

Whitesell, L., and Lindquist, S.L. (2005). HSP90 and the chaperoning of cancer. Nat. Rev. Cancer *5*, 761–772.

Young, J.C., Moarefi, I., and Hartl, F.U. (2001). Hsp90: a specialized but essential protein-folding tool. J. Cell Biol. *154*, 267–273.

Young, J.C., Hoogenraad, N.J., and Hartl, F.U. (2003). Molecular chaperones Hsp90 and Hsp70 deliver preproteins to the mitochondrial import receptor Tom70. Cell *112*, 41–50.

Young, J.C., Agashe, V.R., Siegers, K., and Hartl, F.U. (2004). Pathways of chaperone-mediated protein folding in the cytosol. Nat. Rev. Mol. Cell Biol. *5*, 781–791.